The Dhaka University Journal of Earth and Environmental Sciences, Vol. 13 (1): 2024

Establishing the Relationship between Spatial Distribution of Land Covers and Air Quality: A Case of Coastal Area of Bangladesh

Md. Shakib Al Fahad, Asib Ahmed* and K.M. Nafee

Department of Geography and Environment, University of Dhaka, Dhaka 1000, Bangladesh

Manuscript received: 31 January 2024; accepted for publication: 18 September 2024

ABSTRACT: Employing a GIS-RS integrated approach, the research assesses the concentrations of air quality parameters including nitrogen dioxide (NO_2), sulfur dioxide (SO_2), carbon monoxide (CO), and Aerosol Optical Depth (AOD) across different land cover features in the south-central coastal area of Bangladesh over a six-year period. It also investigates the seasonal variation in air quality parameters. The study reveals that high level of CO and NO_2 concentration was seen across built-up and agricultural areas. Across waterbodies high level of SO_2 and AOD concentration was found. Further analysis reveals a consistent increase in NO_2 concentration, especially in winter seasons with the lowest values at 0.000021 mol/m^2 in 2019 and the highest at 0.000064 mol/m^2 in 2023. Moreover, SO_2 exhibits fluctuating patterns with highest level of concentration being observed in the winter seasons (i.e., 0.0001384 to 0.0005533) mol/m^2. Similar pattern was observed in seasonal CO concentration levels, while AOD concentrations depicts a different picture with high level of concentration observed across monsoon seasons. The study addresses the knowledge gap of identifying high pollution concentration zones across land cover features in the study area. It also provides valuable insights into the seasonal variations of air quality parameters in the study area.

Keywords: Air Quality; Development Impact; Coastal; Google Earth Engine; Remote Sensing

INTRODUCTION

Coastal areas are known for their economic advantages where populations and economic activities are concentrated, therefore playing a vital role in fostering a progressive economy (Mikhaylova et al., 2021). These regions display natural mechanism that enhances biodiversity and sustain population highlighting the significance of global sustainability and conservation efforts (Williams et al., 2021). However, these regions face severe strain due to excessive exploitation and improper management which degrades the operational integrity of coastal ecosystem and the livelihoods of its inhabitants (Ayyam et al., 2019). Therefore, it is imperative that there remains a balance between the developmental undertakings and the natural processes of coastal ecosystem to achieve sustainability (Ayyam et al., 2019). Coastal areas encounter diverse forms of pollutions, such as contamination from polycyclic aromatic hydrocarbons (PAHs), plastic wastes, micro plastic pollution, and the presence of heavy metals and petroleum hydrocarbons (Dai et al., 2022; Chowdhury et al., 2021; Pavithran, 2021; Chitrakar et al., 2019). The issue of air pollution in coastal zones is a serious issue due to its negative implications to both human well-being and ecosystems. Coastal regions, particular those in close proximity to maritime centers, are identified as centers of environmental pollution resulting from various human activities (Piazzolla et al., 2021). Development sector plays a key role in coastal air pollution (Akhter and Das, 2019). Development activities, exemplified by erection of edifices, thoroughfares, harbors and manufacturing plants, can emit a broad spectrum of substances in the atmosphere namely particulate matter 2.5, nitrogen oxides, sulfur oxides, carbon monoxide and ozone. Power plants and various industries are emitting pollutants that expand national and global air quality regulations. The most significant pollutants released from power plants that use coal as their fuel are Sulphur oxides (Sox), Nitrogen oxides (NOx), Particulate Matter (PM) and mercury (Hg) (Sahu et al., 2019). Moreover, the power plant that rely on coal as their source of energy produce greenhouse gases like CO_2 and CO, which have impact on climate. Several development sectors produce a substantial quantity of atmospheric contaminants, which includes the discharge of sulfur dioxide, nitrogen dioxide, and particulate matter (Arif et al., 2019). The discharge of these sectors can result in adverse effects

*Corresponding author: Asib Ahmed

Email: asib01geo@du.ac.bd

DOI: https://doi.org/10.3329/dujees.v13i1.77578

on the wellbeing of individual and the surroundings. The emission of harmful substances from transportation sector cause air pollution of coastal areas (Qi et al., 2020). Pollutants from the air can get deposited in the ocean, leading to acidification and eutrophication.

A number of researchers (Belousov & Tikunov, 2022; Piscopo et al., 2022; Al-Alola et al., 2022; Ahmed et al., 2023;) have highlighted the importance of incorporating an integrated GIS and remote sensing-based approach in air pollution studies. This technological approach in air pollution studies facilitate in illustrating emissions linked to traffic, identifying its distribution and simulates the changes in transportation and land use policies influence air quality (Talib & Jasim, 2021). The geographic information systems (GIS) act as a handy tool to analyse atmospheric air pollution data, allowing for the development of software and cutting-edge technologies that enable proper assessments of air pollution levels (Collins, 2020). These assessments prove vital in providing valuable insights into the spatial distribution of air pollution along with identifying zones having high contamination levels (Rajkumar et al., 2023).

Air pollution along the coast has emerged as a significant global issue, and Bangladesh is currently experiencing the same challenge (Salam et al., 2021; Pavel et al., 2021). Coastal air pollution in Bangladesh is a growing concern as the number of industries along the coast and the increasing number of vehicles on the road are primary sources of coastal air pollution. This pollution has a significant impact on the health of people living in coastal areas and the country's marine ecosystems (Arif et al., 2019). In the context of Bangladesh, geospatial based investigation in air pollution studies have gained popularity. Several researchers have used GIS technologies to craft air pollution monitoring system and assess the concentration of pollutants (Auvee, 2019). Zaman et al., (2021) used GIS technology and spatial analysis to assess, determine the level of aerosol content along with studying its sources and seasonal variations. GIS based approach was used in study of Qiu et al., (2021) to assess the spatiotemporal changes in air pollution that includes particulate matter as well as other gases during the COVID 19 lockdown in major cities of Bangladesh. Faisal et al., (2022) utilized GIS-RS based approach to estimate aerosol optical depth and assess $PM_{2.5}$ concentrations in Dhaka Metropolitan Area (DMA). Hasan and Ahmed (2023) assessed air quality in the coastal area of Bangladesh using an integrated GIS and remote sensing-based approach. However, no previous studies in this domain assessed the concentration level of air quality parameters across different land cover features in the coastal area of Bangladesh. Assessing air quality parameters over different land cover features facilitates the identification of pollution sources in specific land cover features, enabling the foundation for evidence-based decision-making for managing air pollution.

Observing the development trend in the coastal region of Bangladesh it is evident that rapid shift in land use pattern has occurred in the past few decades signaling a change in the concentration of various components of air. Therefore, present study focuses in assessing the air quality of south-central coastal areas of the country. The specific objectives of the study include:

1) The quantification and assessment of the concentration of AOD, nitrogen dioxides, sulfur dioxides and carbon monoxide across different seasons over 6-year period in the south-central coastal area of Bangladesh.

2) Identification of specific land cover classes with high concentration levels of AOD, Nitrogen dioxides, sulfur dioxides and carbon monoxide.

The significance of this research lies in its potential contribution towards addressing the gap of knowledge pertaining to proper identification of particular land cover classes exhibiting high level of pollution. By identifying specific land cover classes associated with high level of pollution, the study provides evidenced based information essential for effective air pollution management and mitigation strategies in the study area. Additionally, the study seeks to provide valuable insights into the dynamics of air quality over different seasons, offering a deeper perspective into the pattern of air pollution.

MATERIALS AND METHOD

The method employed in this research was a cross-sectional approach to gather information concerning the current levels of air pollution prevalent in the area under examination. Information pertaining to air quality was gathered and assessed during a particular timeframe to identify the extent of air contamination within the study area. Information regarding the levels of diverse atmospheric contaminants was gathered using Sentinel

5P satellite and Terra and Aqua MODIS images. Land cover was determined by Landsat 8 Collection 2 TOA Reflectance (Figure 1). The data were analyzed for individual zones after the study area had been segmented into multiple sections. Subsequently, resampling was applied to the data, and seasonal variation maps and land cover maps from 2018 to 2023 were generated. Following this, the obtained data were validated.

Nitrogen dioxide (NO2), sulfur dioxide (SO2), carbon monoxide (CO), and Aerosol Optical Depth (AOD) data were collected from the published work of Hasan and Ahmed (2023) in order to validate the results of the present study. Random points were generated, values were extracted from the data, and these values were compared with the results of the present study. Python Scripts were developed by Jupyter Notebook to generate the observed data under various statistical parameters in order to observe the correspondence between the data generated in the study and the published data.

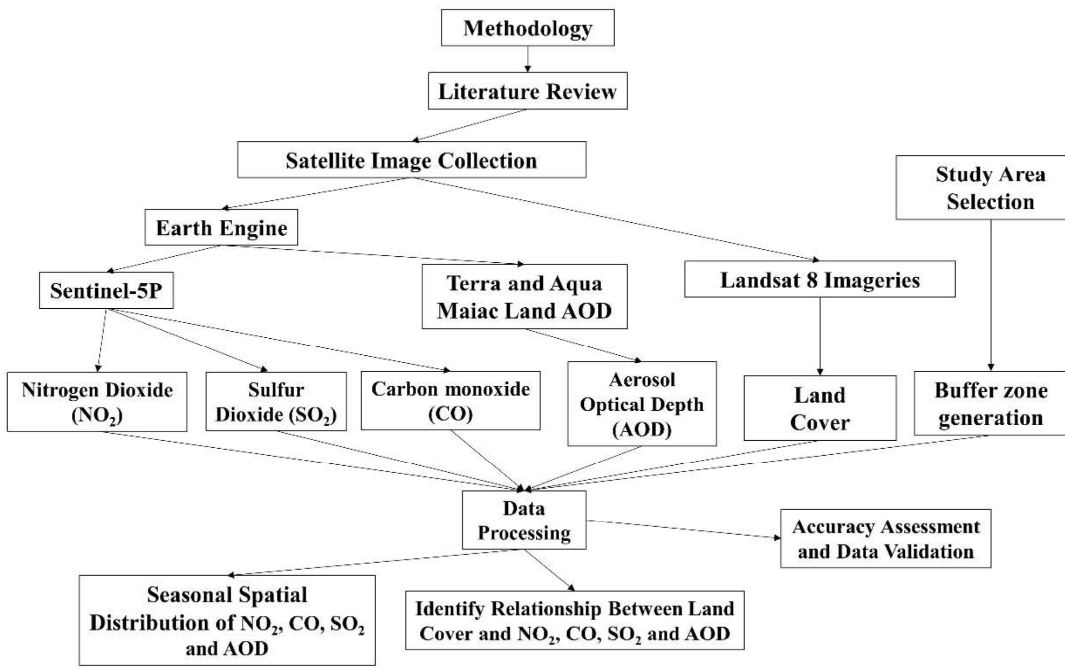

Figure 1: Flowchart Depicting the Research Methods Applied for the Present Study

Study Area

In the present study, the area selected was in and around Payra Port and the Coal Power Plant, located in the south-central coastal zone of Bangladesh, to identify the nexus between development activities and changes in air quality. The construction of Payra Port and the establishment of the Payra 1320 MW thermal power plant in the southern part of Barishal division have had a significant impact on the coastal development of the south-central region. These two features are located on the banks of the Payra River in Patuakhali district (Tareq et al., 2020). The emergence of these massive structures has accelerated the process of industrialization and urbanization in the region. Based on the location of these two structures, a circular buffer influence zone was created to examine air quality (Figure 2). Five concentric zones were generated with radii of 3 km (1st Zone), 6 km (2nd Zone), 12 km (3rd Zone), 24 km (4th Zone), and 48 km (5th Zone). Circular buffers provide a more detailed geographic depiction of possible hazards than spatial coincidence since the negative impacts are not restricted to the host spatial unit limits (Chakraborty et al., 2011).

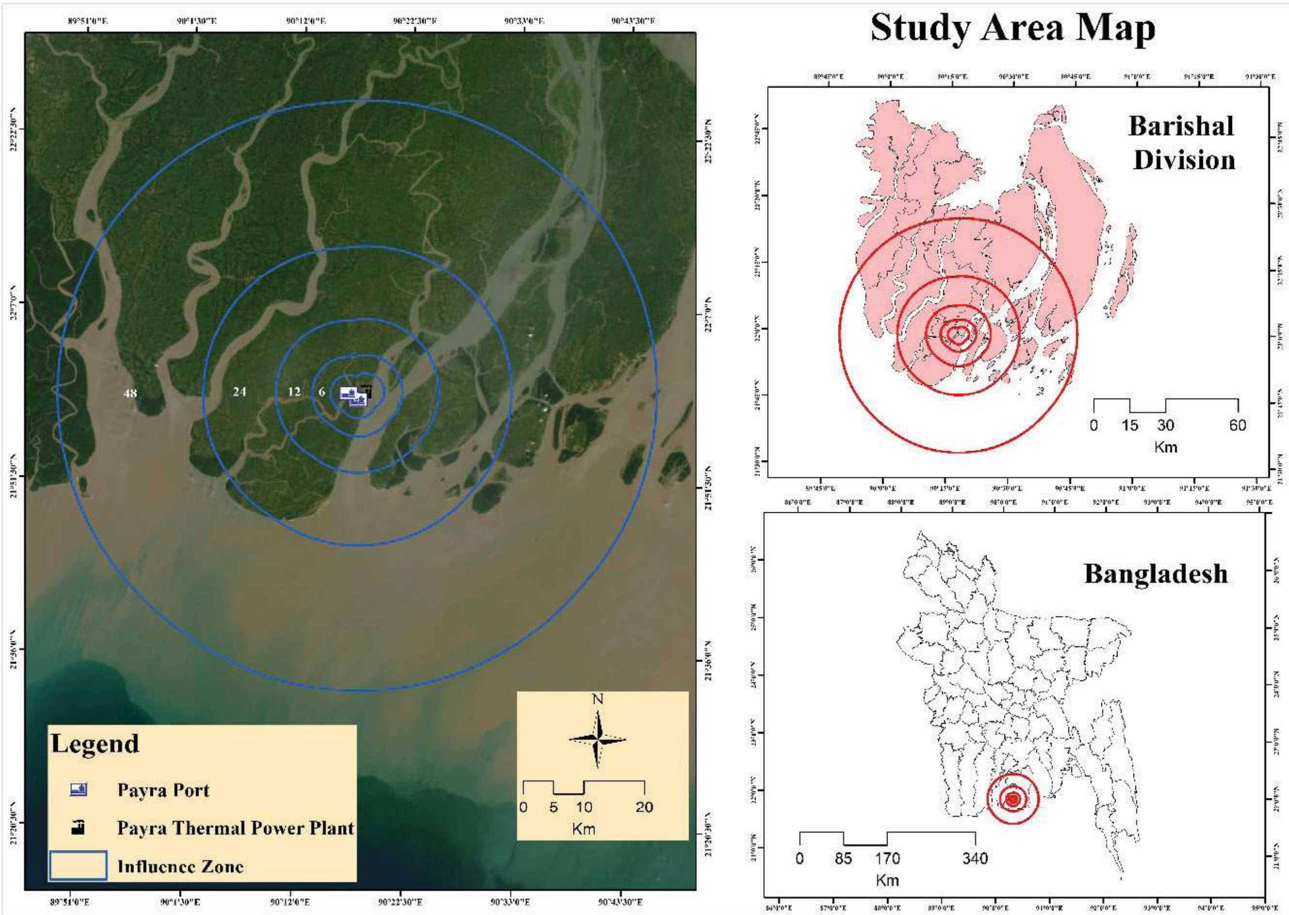

Figure 2: Payra Port, Coal Power Plant, and their Sphere of Influence in the Selected Study Area

Data Collection

During this study, information regarding the levels of air pollution in specific areas was obtained utilizing satellite imagery. Satellite images from Sentinel 5P were obtained through Google Earth Engine. Analysis was facilitated by Google Earth Engine through a cloud-based platform that provides access to ample geospatial data and computing power. Codes were appropriately developed through JavaScript language to extract and mask various contaminants, such as nitrogen dioxide (NO2), sulfur dioxide (SO2), aerosol optical depth (AOD), and carbon monoxide (CO). To identify seasonal variation of air pollution, the air pollution data were collected across four seasons classified as Pre Monsoon (March, April, and May), Monsoon (June, July, August, and September), Post Monsoon (October and November), and Winter (December, January, and February) following the Bangladesh Meteorological Department's classification. Data from Landsat 8 Collection 2 Tier 1, which captures top-of-atmosphere information, were also utilized. Data were gathered on several occasions during the designated time frame in order to account for the fluctuation of air pollution levels over time and for assessing land cover.

Table 1: Dataset in Details which are used in Analysis

Data Type	Name of Dataset	Source	Specifications of Processed Data
Raster	Nitrogen dioxide (NO2)	Image Collection (COPERNICUS S5P NRTI L3_NO2)	30 m resolution
	Sulfur dioxide (SO2)	Image Collection (COPERNICUS S5P NRTI L3_SO2)	30 m resolution
	Fine particulate matter (PM2.5)	Image Collection (MODIS 006 MCD19A2 GRANULES)	30 m resolution
	Carbon monoxide (CO)	Image Collection (COPERNICUS S5P OFFL L3_CO)	30 m resolution
	Land Cover	Satellite Image Collection (LANDSAT/LC08/C02/T1_TOA)	30 m resolution
Vector	Administrative Boundary	BBS 2021	Line and Polygon shape file format

Data Preparation

Preparation of different Air Pollutant Data

The different air pollutant datasets offered a spatial resolution of 7x3.5 km, indicating that every pixel displayed on the image corresponds to an approximate area of 7x3.5 square kilometers. However, to analyze air pollution patterns and establish its relationship with different land cover classes within a smaller area of focus, a spatial resolution of 30 meters was required. To meet the resolution needs, data resampling techniques were employed, involving adjustments to the pixel size to better suit the study's objectives.

Buffer Zone

The process of buffer generation, which creates additional polygons around point, line, or polygon features, is a common analytical function in many GIS software programs. It is frequently utilized to analyze the attributes of the locations of environmental risks (Chakraborty and Armstrong, 1997). Nevertheless, alternative studies propose that GIS technology be used to create circular buffers around toxic emission sites as a more logical approach to depict affected neighborhoods and associated hazards (Glickman, 1994; Zimmerman, 1994; Glickman and Hersh, 1995). It was argued that political or administrative boundaries cannot accurately depict the size and shape of the potentially impacted area of a hazardous facility, supporting the use of the buffer methodology. Five buffer zones were created around the center point of Payra Port and the Payra Ultra Super Power Plant to pinpoint the areas with the highest contamination levels. These zones were set up in ArcMap 10.3 with the following diameters: 3 km for the first, 6 km for the second, 12 km for the third, 24 km for the fourth, and 48 km for the fifth.

Preparation of Land Cover Map

Six maps of land cover were created using the supervised classification technique employing the maximum likelihood algorithm. A multi-sectoral supervised classification algorithm was used to generate land cover maps for specific years (Lucas et al., 2007). Satellite images from Landsat 8, containing seven bands, were combined to create a composite image (Zha et al., 2003). Before conducting supervised classification, various preparatory steps had to be taken: composite bands were generated, raster data duplicated, clouds eliminated, merged into a new raster, extracted through masking, and maximum likelihood classification was applied (Su et al., 2010). The tasks were carried out utilizing ERDAS IMAGINE and ArcMap 10.3. The extract by mask tool (Magesh and Ch, 2012) was used to extract specific locations. During the training process, a large number of pixels were chosen for different land cover categories, with approximately 450 training data sets allocated for each class. The supervised classification method based on maximum likelihood was applied in ArcMap 10.3.

Data Analysis

Identification of Air Pollution Pattern

Data from the Sentinel 5P and Landsat 8 satellite images, collected through the Google Earth Engine platform, were carefully reviewed using Geographic Information System (GIS) software. Maps of the research area were created by using Geographical Information System (GIS). Concentration levels of each air quality parameter were assessed across the study area through extraction and subsequent spatial analysis to understand the distribution and intensity of concentration levels of these pollutants. The information obtained was then used to compute and map the concentrations of various air pollutants across different seasons.

Establishing Relationship between Land Cover Classes and Air Pollution

The land cover data generated from supervised classification were initially converted into polygon files using the conversion tool, and different classes were separated from the data. Each separated class of land cover data was subsequently employed as a mask to isolate the corresponding regions in the air pollutant layer files. The average pollution levels within these specific land cover classes were then observed and recorded.

The methodology adopted in the study was well-suited for analyzing air pollution patterns through its multi-layered approach. Integration of high-resolution satellite imagery with GIS-based spatial analysis made it highly effective for evaluating pollution levels and relating them with land cover types. The approach captures specific pollutant levels within the concentric buffer zones, designed to represent the spread of pollution gradients more accurately than administrative boundaries. The use of Google Earth Engine to gather pollutant data across different seasons allowed for an enhanced understanding of pollution levels, enabling the detection of subtle changes in air pollution levels across different pollutants. Land cover classification allowed identifying how pollution levels correlate with different land cover types. This integrated and multi-layered approach permitted an assessment of pollution patterns, making it highly adaptable for environmental monitoring and assessment in complex, dynamic regions.

RESULT

Analysis of seasonal and temporal variation in air pollutants (NO_2, SO_2, CO, and AOD) in the study area, highlight spatial distribution and concentration trends over a six-year period. The seasonal division was taken according to Ahasan et al., (2010) where Post-monsoon lasts from October to November, Winter lasts from December to February, pre-monsoon lasts from March to May, and monsoon lasts from June to September.. Additionally, a land cover classification assessment was conducted to evaluate the relationship between land use changes and pollutant distribution. Accuracy assessments were performed using the Cohen's Kappa coefficient, mean percent error (MPE), Mean Aboslute Error (MAE) and root mean square error (RMSE) to validate the stuyd's data against existing published datasets.

Nitrogen Dioxide

According to data collected from 2018 to 2023, there has been a steady rise in the concentration of Nitrogen Dioxide (NO_2). This increase is most pronounced during the winter season, with the highest levels of NO_2 recorded during this time. Conversely, the levels of NO_2 are generally lower during the monsoon season. A notable observation in the winter of 2022 was that both the northern and central areas of the studied region experienced exceptionally high levels of NO_2, which remained elevated throughout the post-monsoon and pre-monsoon seasons.. The mean value of concentration level of Nitrogen Dioxide around 3km area over the port and the power plant substantially increased from 0.0000247 mol/m^2 0.0000566 mol/m^2 over 6 years signaling the susceptibility of these areas to the accumulation of NO_2.

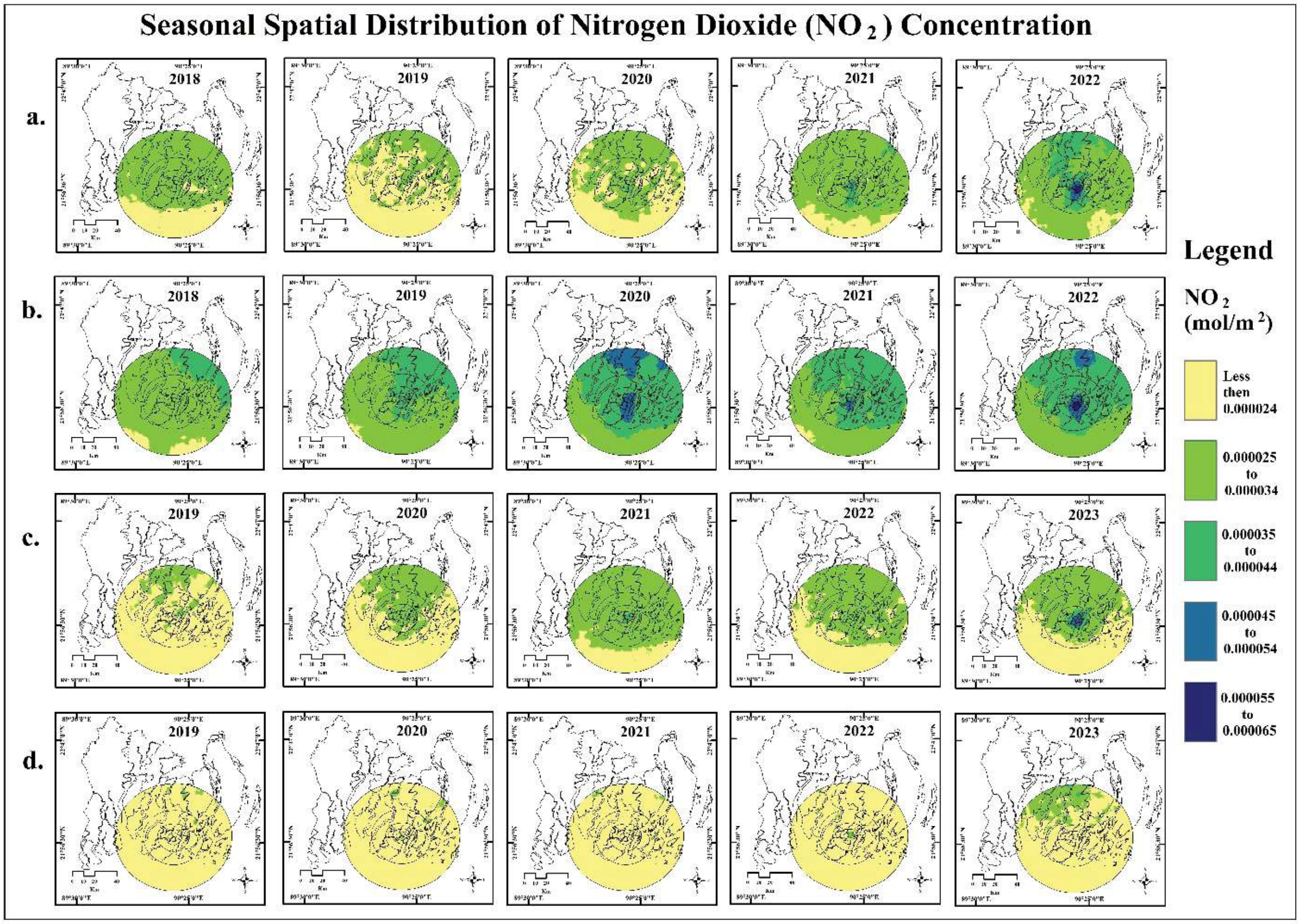

Figure 3: Seasonal Spatial Distribution of Nitrogen Dioxide (NO_2). a) Post-monsoon Seasons, b) Winter Season, c) Pre-monsoon Season, d) Monsoon Season.

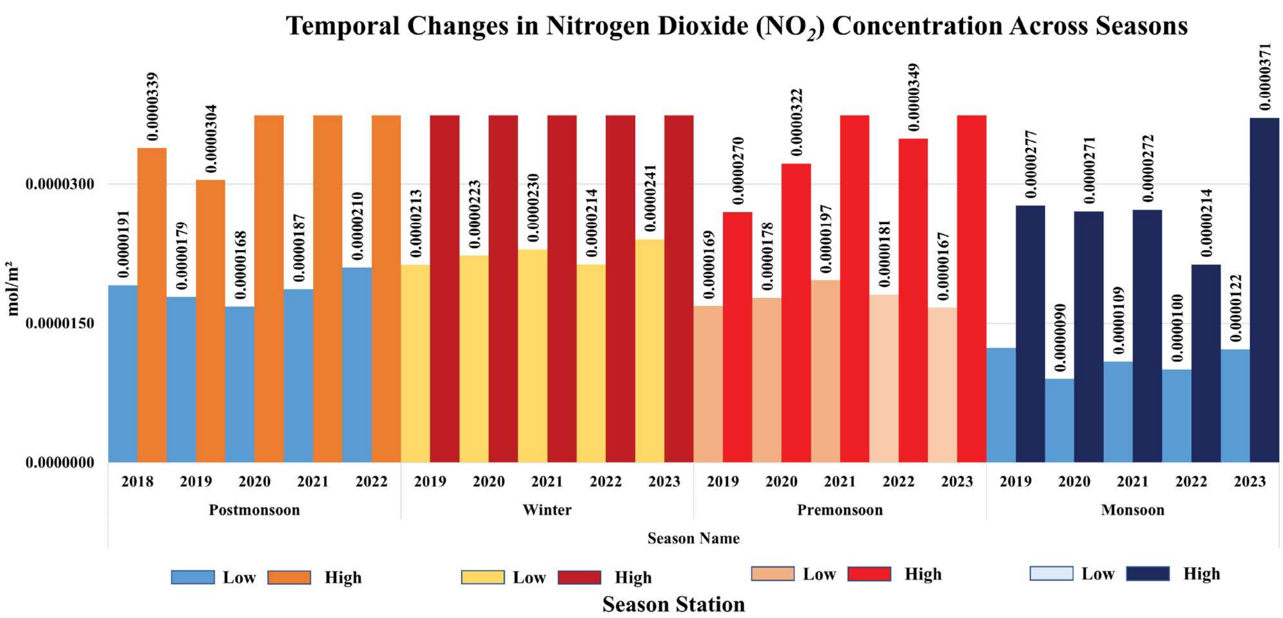

Figure 4: Seasonal Variations in Nitrogen Dioxide (NO_2) Concentrations over the Years

Air quality patterns for Nitrogen Dioxide levels vary across different seasons and years. From 2018 to 2022, NO_2 levels decreased during the monsoon season, dropping from 0.000019 to 0.0000021 mol/m² at low points, and from 0.000034 to 0.000062 mol/m² at high points. During winter seasons, the overall NO_2 concentration level increased over the same period, with low points rising from 0.0000213 to 0.0000241 mol/m² and high points rising from 0.0000404 to 0.0000643 mol/m². In the pre-monsoon period, NO_2 levels fluctuated between 0.0000167 and 0.0000197 mol/m², while the high values indicated a rising pattern from 0.0000270 to 0.0000556 mol/m².A similar pattern is also observed in the post-monsoon seasons where the concentration levels of NO_2 gradually increased at both high and low points over the years.

Sulfur Dioxide

During the timeframe spanning from 2018 to 2023, there were noticeable differences in sulfur dioxide (SO_2) concentration patterns between various seasons. The winter and pre-monsoon seasons consistently display the higher concentration levels, while the levels of concentration are consistently becoming lower during the post-monsoon and monsoon seasons. Sulfur dioxide (SO_2) is distributed across the terrestrial and aquatic realms. Sulfur dioxide is emitted through maritime transportation. The southern-central region's coastal area functions as a significant thoroughfare for transportation via maritime means. Analyzing the data of Sulfur Dioxide concentration level in the study area it was found that lower concentration levels of SO_2 existed during the monsoon seasons with average value 0.00019 mol/m². Higher concentration level of SO_2 was observed during the winter seasons with average value of 0.0051 mol/m². .

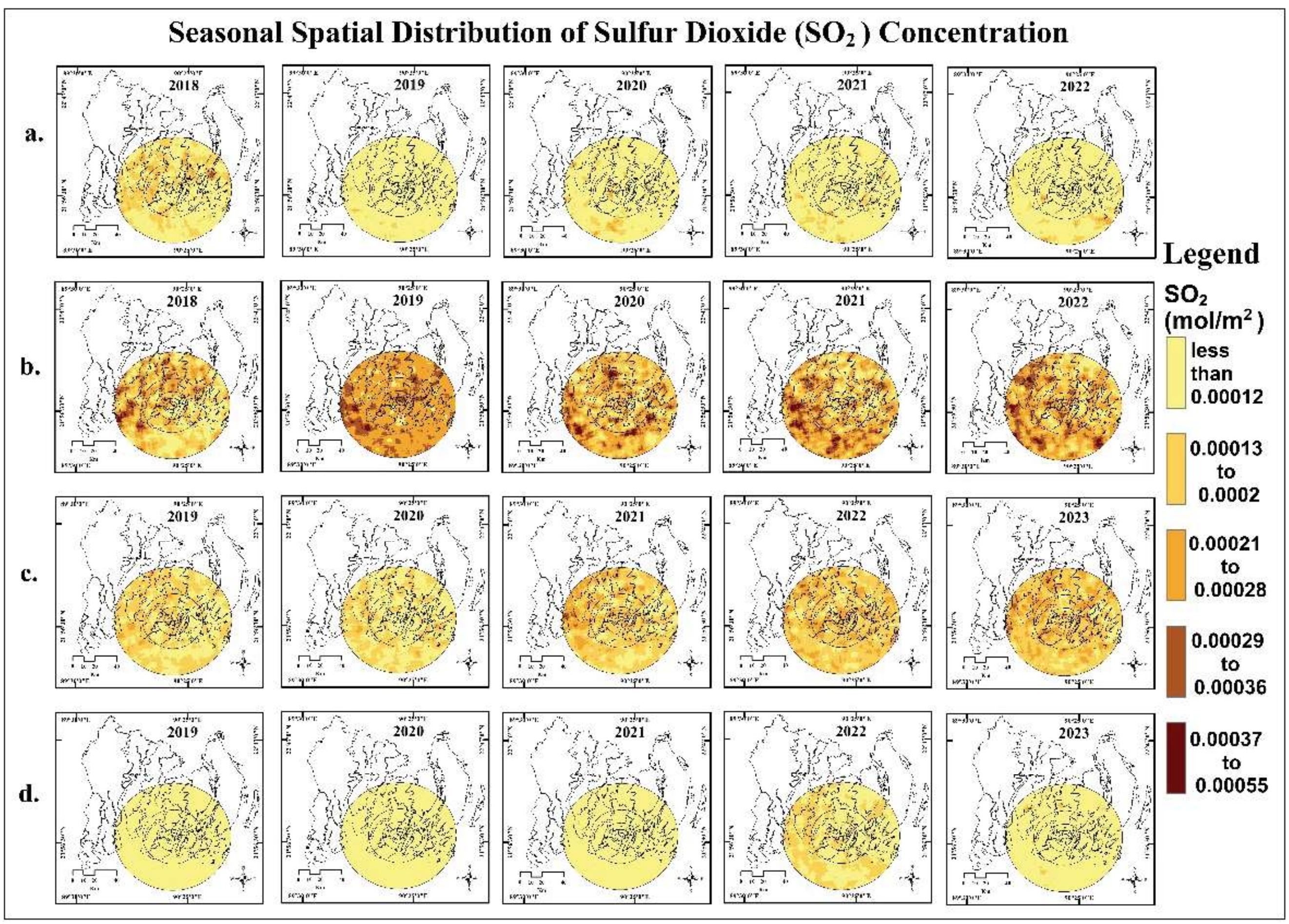

Figure 5: Seasonal Spatial Distribution of Sulfur Dioxide (SO_2). a) Post-monsoon Seasons, b) Winter Season, c) Pre-monsoon Season, d) Monsoon Season

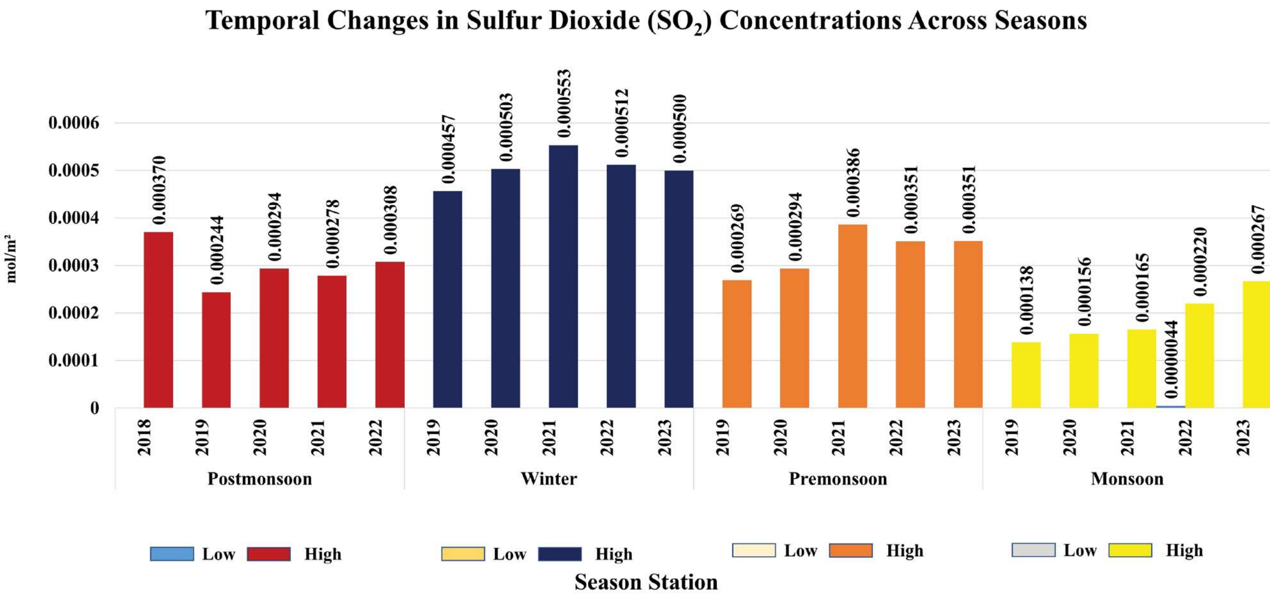

Figure 6: Seasonal Variations in Sulfur Dioxide (SO_2) Concentrations over the Years

The concentrations of SO_2 in post-monsoon season showed a decreasing pattern with concentration levels varying from 0.00370 mol/m^2 in 2018 to 0.00308 mol/m^2. During winter season, fluctuations of the concentrations levels of SO_2 was observed. . During this period SO_2 values varied from 0.000456713 mol/m^2 in 2019, and 0.000503 mol/m^2 in 2020. The value for the year 2021 was 0.0005119 mol/m^2, and it climbed to 0.000553 mol/m^2 in 2022 and later on to 0.0005 mol/m^2 in 2023. . In pre-monsoon season, the concentration level of SO_2 was 0.000269 mol/m^2, and in 2020, it rose to 0.000294 mol/m^2.From 2021 a declining pattern was observed in the concentration level of SO_2 with values dipping from 0.000385 to 0.00351 mol/m^2 by 2023.

Sulfur dioxide concentration was found to be the lowest across all monsoon season over the six-year period. The values ranged from 0.000138 mol/m^2 in 2019 to0.000267 mol/m^2 in 2023 indicating a rising trend. The lower values of sulfur dioxide were considered as zero due to the noise of the dataset of Sentinel-5p Sulfur dioxide data yielded negative column values over the region of the study area. This is a limitation of the dataset of sulfur dioxide obtained from Sentinel 5p.

Carbon Monoxide

In 2018, the highest values of carbon monoxide concentration were noted over land surfaces, marking an observable peak. Moving into 2019, high levels of carbon monoxide levels were observed in the 5th zone and in the 4th zone, both showing mean value approximately 0.045 mol/m^2 which exhibited higher concentrations compared to other areas. However, 2020 witnessed an overall reduction in carbon monoxide concentration across terrestrial regions with across all seasons being 0.0415mol/m^2, signaling a clear decrease from previous years. In 2021, a notable rise in carbon monoxide concentration was recorded within the sea surface region, indicating elevated oceanic levels compared to preceding years. Conversely, 2022 saw high level of carbon monoxide concentration above terrestrial zones, with land-based levels comparatively lower than those over the sea. Looking ahead to 2023, there's a discernible increase in the upper limit of carbon monoxide concentration ranging from 0.037 to 0.056 mol/m^2 across four different seasons, hinting at a potential upward trend across land surfaces compared to previous years.

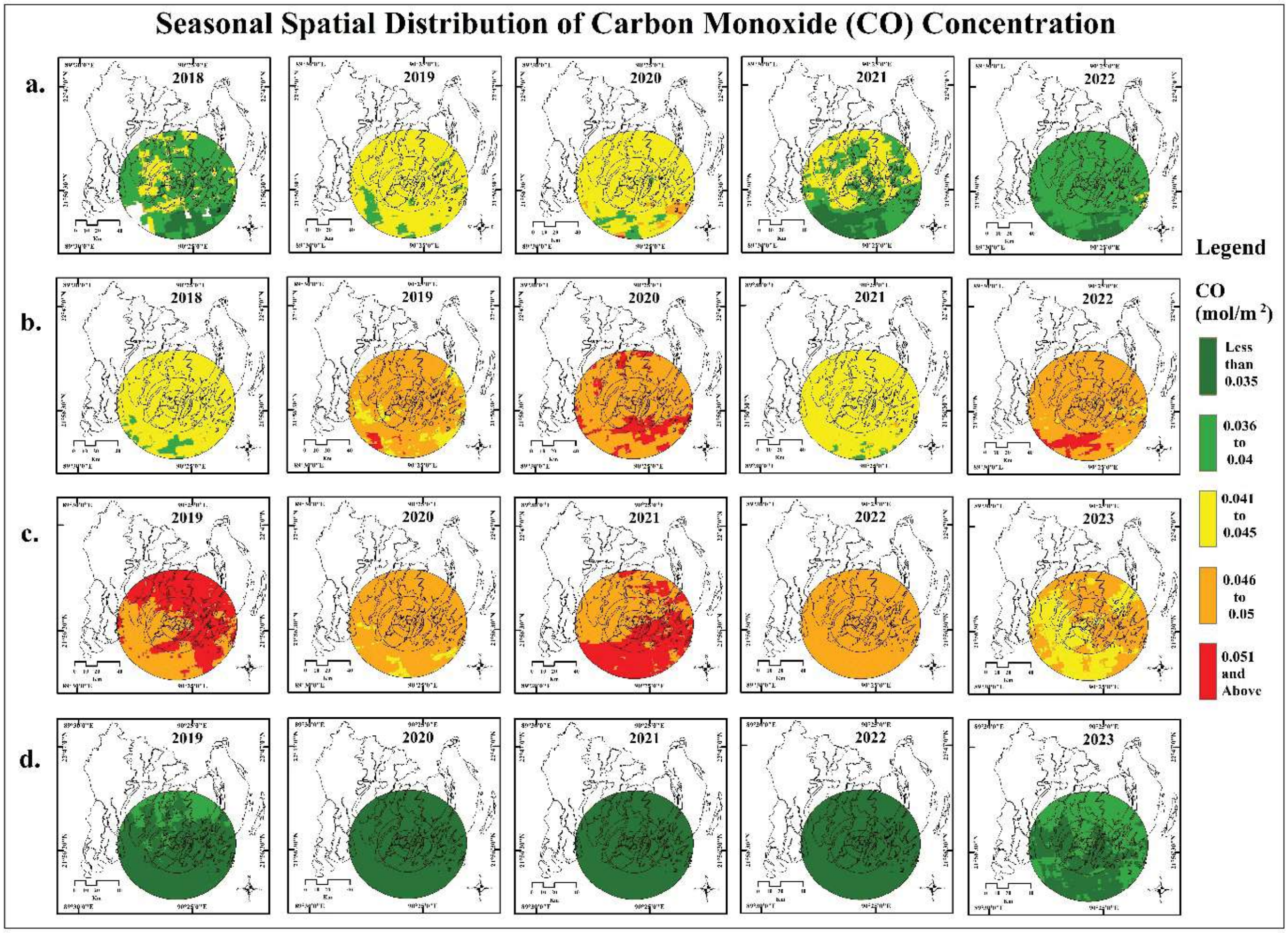

Figure 7: Seasonal Spatial Distribution of Carbon Monoxide (CO). a) Post-monsoon Seasons, b) Winter Season, c) Pre-monsoon Season, d) Monsoon Season

Concentration levels of Carbon Monoxide (CO) across the study area indicate a seasonal variation, with lower concentration levels being observed during the monsoon season and the higher concentration levels being observed in the pre-monsoon season. During monsoon season, the average concentration levels across the timeline of the study ranged from 0.032 to 0.035 mol/m^2. In pre-monsoon from 2019 to 2023, the mean concentration levels of CO ranged between 0.045 and 0.046 mol/m^2, peaking at 0.05 mol/m^2 in 2021. In winter, CO mean concentration levels showed a gradual increase over the years from 0.043 mol/m^2 in 2018 to 0.047 mol/m^2 in 2022. Post monsoon carbon concentration level showed fluctuation over the years with mean concentration values decreasing from 0.038 mol/m^2 in 2018 to 0.037 mol/m^2 by 2022. However, the concentration levels peaked in the year 2020 with mean value reaching to 0.042 mol/m^2.

Aerosol Optical Depth (AOD)

During 2018, elevated levels of AOD were observed in proximity to the riverbank and in the western area, a trend that extended across the sea surface and the western side of the influence zone throughout the year. This AOD pattern persisted through 2020. In 2022, a significant concentration phenomenon emerged in the southwestern region. Current data for 2023 indicates a continuation of concentration patterns within the influenced area. The higher concentration levels are noted during the winter and pre-monsoon seasons, while the lower levels are observed during the post-monsoon and monsoon periods.

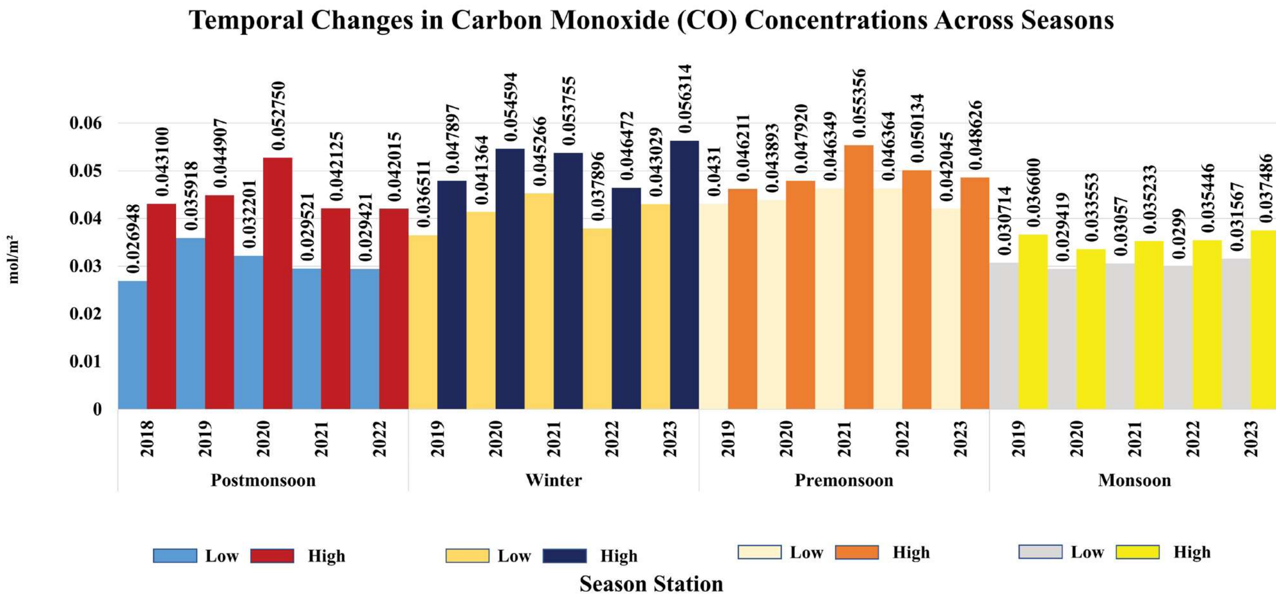

Figure 8: Seasonal Variations in Carbon Monoxide (CO) Concentrations over the Years

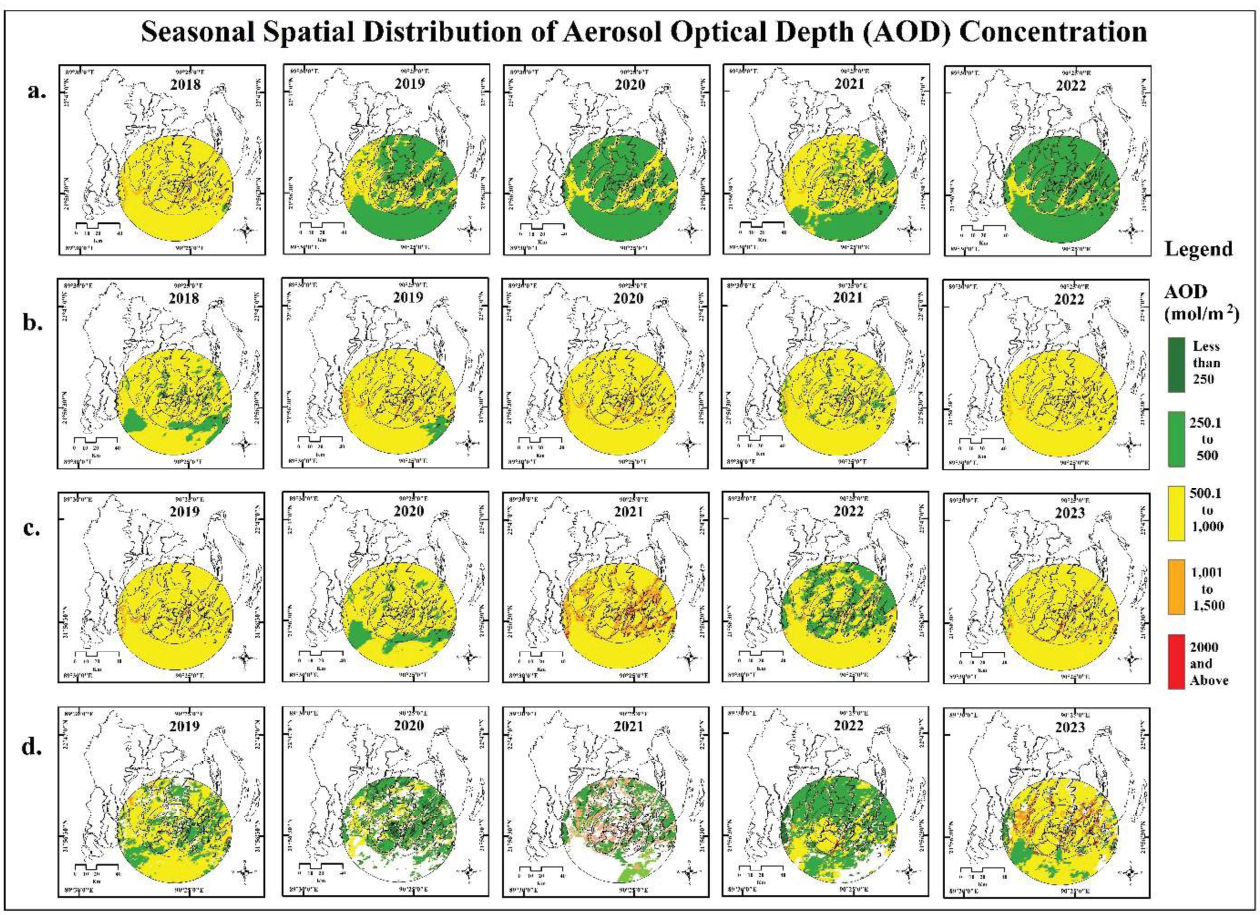

Figure 9: Seasonal Spatial Distribution of Aerosol Optical Depth (AOD). a) Post-monsoon Seasons, b) Winter Season, c) Pre-monsoon Season, d) Monsoon Season

AOD mean concentration level showed a gradual increase from 571.81 mol/m^2 in 2019 to 739.96 mol/m^2 by 2023 in Monsoon season. AOD mean concentration level in winter also exhibited gradual increase from 563.29 mol/m^2 in 2018 to 762.97 mol/m^2 by 2022, with a steep rise of 818.78 in 2020. A reverse pattern was observed in the mean concentration levels of AOD which drastically decreased over the years in the post-monsoon season from 737.83 mol/m^2 in 2018 to 449.21 mol/m^2 by 2022. In the pre-monsoon seasons, the average concentration level increased with values rising from 718.97 mol/m^2 in 2019 to 744.99 mol/m^2 by 2023. However, instances of sharp rise and steep decline was also witnessed during this period especially in 2021 when the average concentration level increased to 897.55 mol/m^2 and in the next year dipped to 579.55 mol/m^2.

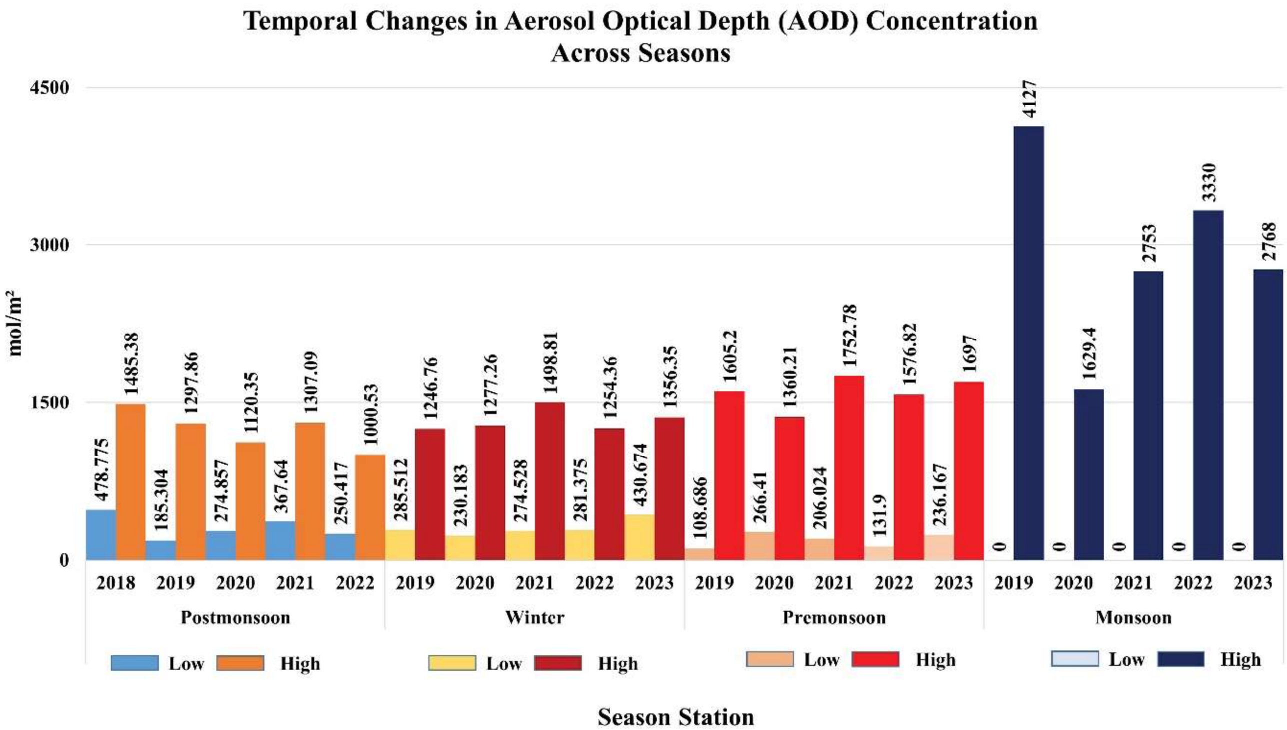

Figure 10: Seasonal Variations in Aerosol Optical Depth (AOD) Concentrations over the Years

Land Cover Class Change throughout the Years

The study area went through considerable land cover changes over the observation period. Built-up area increased from 1.27 percent in 2018 to 3.08 percent in 2023, while agricultural land decreased from 38.71 percent to 36.27 percent over the same time period. Bare land and Waterbody had relatively constant areal coverage across the timeframe of the study. Vegetation class on the other hand, witnessed an increase from 18.56 percent in 2018 to 19.06 percent in 2023.

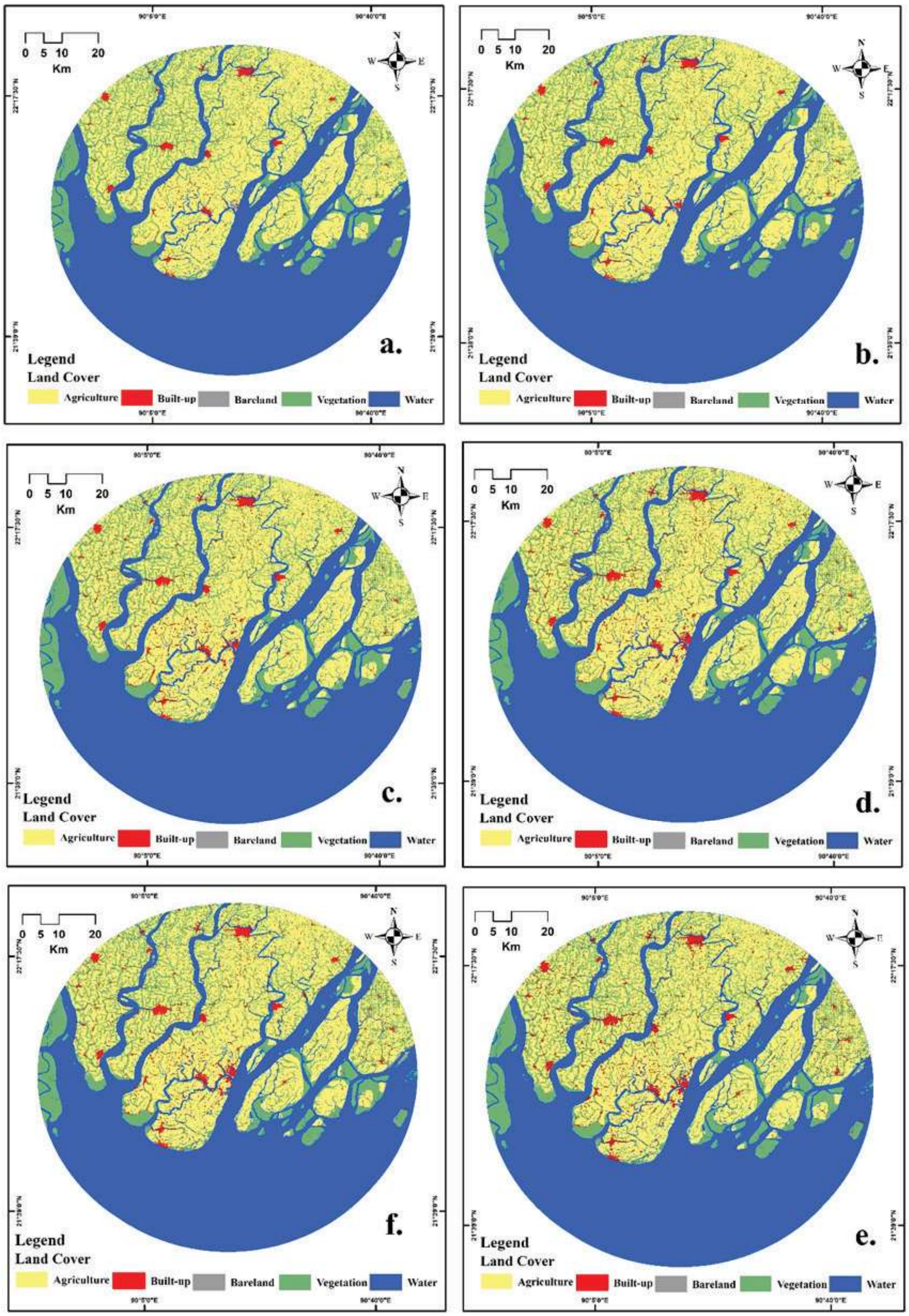

Figure 11: Land Cover in the Study Area from 2018 to 2023: a.2018. b.2019, c.2020, d.2021, e.2022, f.2023

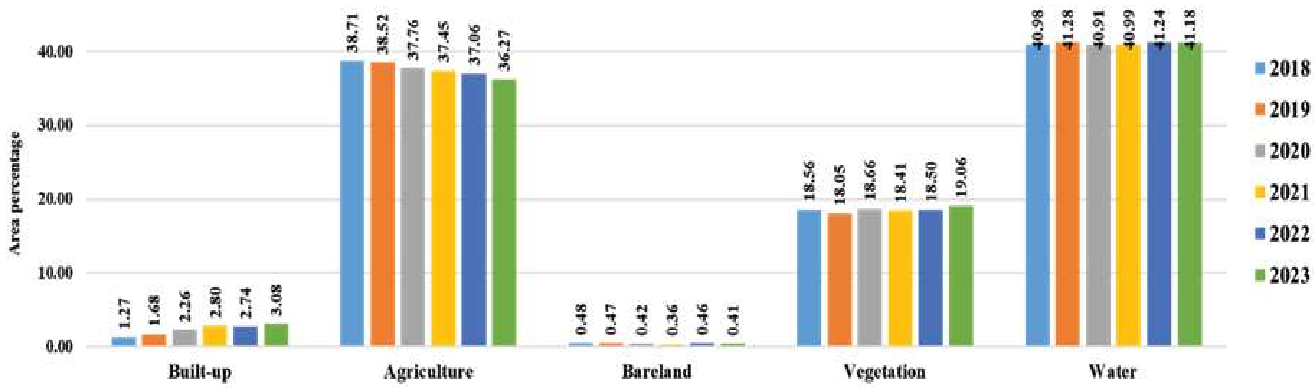

Figure 12: Percent Changes in Land Cover in the Study Area from 2018 to 2023

Accuracy Assessment of Land Cover Maps

In this study, the Cohen's Kappa coefficient served as a metric to evaluate the land cover maps. The overall accuracy of the different land cover maps ranged from 85.33% to 89.37% while the co-efficient value ranged from 0.8292 to 0.8661 which falls within high level of acceptance rate for land cover classification. The individual accuracy metric were generated by extracting point data and comparing the values with real-time data captured from Google Earth Pro images. The user and producer's accuracy were generated for each individual classes as listed in Table (2).

Table 2: Accuracy Evaluation for Land Cover Classifications

	2018		2019		2020		2021		2022		2023	
Land Cover Type	Producer's accuracy (%)	User's accuracy (%)	Producer's accuracy (%)	User's accuracy (%)	Producer's Accuracy (%)	User's accuracy (%)	Producer's accuracy (%)	User's accuracy (%)	Producer's accuracy (%)	User's accuracy (%)	Producer's accuracy (%)	User's accuracy (%)
Agriculture	92.68	92.68	95.08	95.08	94.23	94.23	90.63	90.63	91.18	91.18	87.50	83.33
Built-up	87.50	83.33	89.80	86.27	88.10	84.09	94.38	89.41	91.48	85.86	88.37	86.36
Bareland	88.37	86.36	88.37	86.36	89.58	87.76	88.10	86.05	86.84	89.19	84.78	90.70
Vegetation	84.78	90.70	82.50	89.19	87.04	92.16	82.50	89.19	83.33	89.74	88.10	86.05
Water	83.54	86.54	88.52	85.52	86.50	87.50	87.04	84.04	88.37	84.44	82.50	89.19
Overall Accuracy (%)	87.84		89.37		88.56		86.50		86.41		85.33	
Kappa coefficient	0.8477		0.8661		0.8566		0.8296		0.8292		0.8337	

Air Quality over different Land Cover Class

Observing the mean yearly trend of different air quality parameters in different land cover classes it is seen that CO and NO_2 is highly concentrated across built-up areas in the study area with values 0.0438408 mol/m^2 and 0.00002937 mol/m^2 respectively. Agricultural class also exhibited high concentration levels for these two parameters with mean value over 6-year period was 0.043917953 mol/m^2 for CO and 0.0000287 mol/m^2 for NO_2. On the other hand, high concentration levels of AOD (759.8370468 mol/m^2) and SO_2 (0.000145113 mol/m^2) was found in waterbody class of the study area.

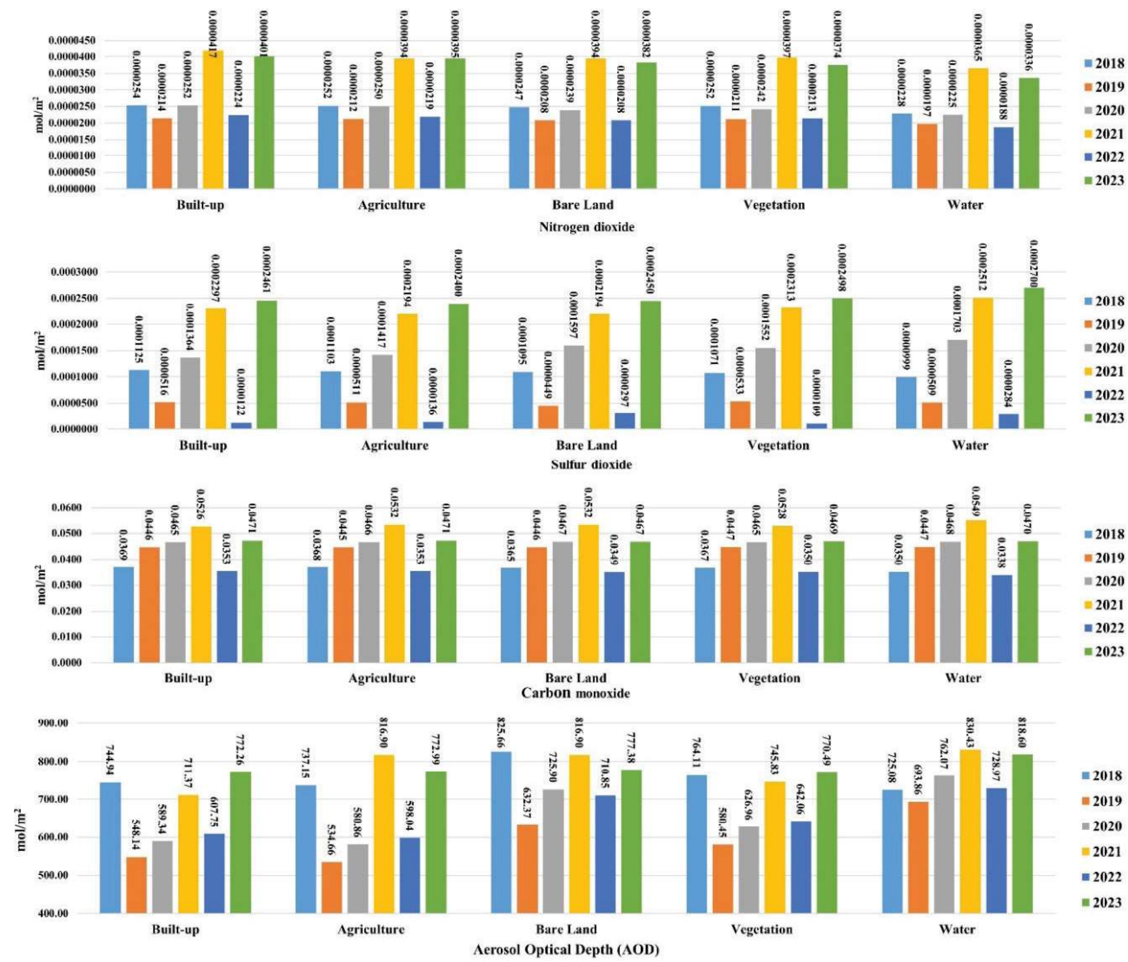

Figure 13: Percentages of Land Cover Changes in the Study Area from 2018 to 2023

Validation of the Results

Table 3: Validation of the Results Under different Parameters Used for the Present Study

Parameters	AOD	CO	NO_2	SO_2
Mean Percent Error (MPE)	1.582	2.44	4.97	2.04
Mean Absolute Error (MAE):	4.86	5.9×10^{-3}	2.12×10^{-3}	2.802×10^{-5}
Root Mean Square Error (RMSE)	2.18	8.3×10^{-3}	0.0041	3.38×10^{-5}

Through the generation of different statistical parameters from the results of the study it is seen that the values of MPE falls below 5 percent indicating that the results displayed fairly good amount of accuracy. Additionally, lower values of MAE and RMSE from the (Table 3) further supports the data in relation to results obtained from published data. Overall, the calculation of MPE, MAE and RMSE shows that the results obtained from the present study matches with the published results reasonably well validating the findings of the study.

Apart from using different parameters, the study attempted to validate the data using generation of random sample over the study area. Comparing the values extracted from different air pollutant datasets of the study and published dataset collected from Hasan and Ahmed (2023) the results of the study were validated. Data analysis revealed that mean difference of Nitrogen dioxide from the published data was 0.00048 mol/m², for Sulfur dioxide the value is 0.000061 mol/m², for Carbon Monoxide the value is 0.0017 mol/m² and for AOD it is 21.86 mol/m². These small mean differences indicate that the study's data closely aligns with the published dataset, thereby validating the accuracy and reliability of the data.

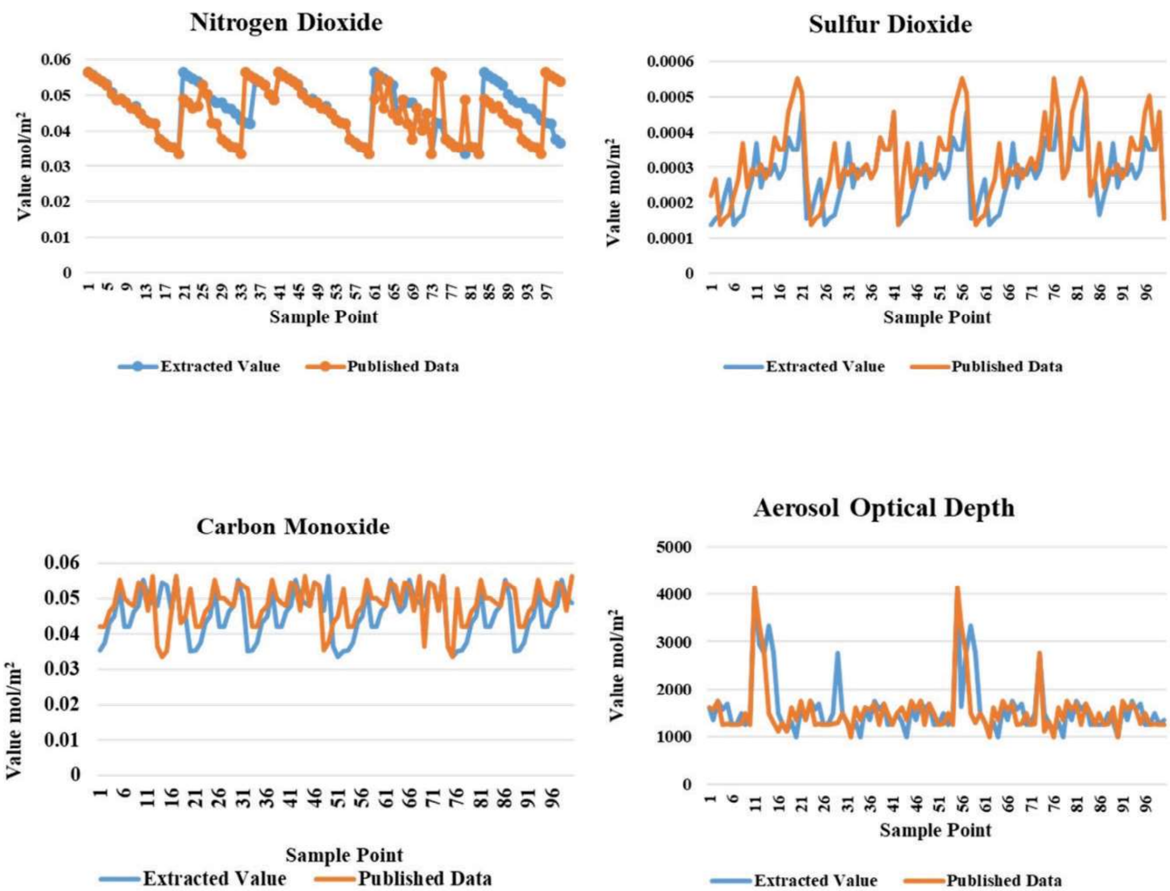

Figure 14: Comparative Analysis of Extracted Values and Published Data

DISCUSSION

Analysis of the results yielded a clear seasonal trend of different pollutant across the study area. The concentration of different air pollutants that is Nitrogen dioxide (NO_2), Carbon Monoxide (CO), Aerosol Optical Depth (AOD) and Sulfur dioxide (SO_2) investigated during the study showed high level of concentration during winter seasons and low concentration during monsoon. Past research suggests that air pollution tend to be high in the winter season in coastal areas due to various factors including wind direction and speed (Wei et al., 2020), ship emission, mineral aerosol, and gaseous pollutant (Bencs et al., 2020), industrial activities, coal combustion and activities of local powerplants (Siudek, 2020). On the other hand, due to increased wind speed and precipitation that aid in dispersing and washing pollutants from the atmosphere contribute to low pollution during monsoon season (Hu et al., 2023; Jayasundara and Elangasinghe, 2022). Apart from that influence of biogenic emissions that reduces fine particulate matter levels also plays a crucial role in reducing pollution during monsoon season(Mogno et al., 2021). Trends derived from the results of our study are in line with those found in previous research. The study area which has a port and coal power plant in the central part exhibit noticeable patterns and trends in different air quality parameter. Observing the yearly trend of the concentration level of these gases in the present study pointed out that there is constant rise of NO_2 and CO in areas over built-up and agricultural land. The expansion of builtup areas leads to increased emissions of NO_2 and CO impacting regional air quality (Dhankar et al., 2024). Additionally, the correlation matrix in the study of Dhankar et al., (2024) is indicative of a strong positive correlation among air pollutants, with NO_2 showing significant correlation with CO, emphasizing the interconnected nature of these pollutants in built environment. High concentrations of NO_2 and CO are found over agricultural lands due to emissions of Nitrogen dioxide from fertilized soils in high-temperature environment (Oikawa et al., 2015). Burning of biofuels and crop residues contribute to elevated CO levels over agricultural areas (Wang et al., 2002). On the other hand, areas over waterbodies exhibited high level of concentration of AOD and SO_2. This observed distribution reflects a complex interplay of multiple factors. The higher AOD and SO_2 concentration level can be associated with increased maritime activities, shipping emission and release of pollutants from marine sources. Since major infrastructures of Payra port serve as a focal point for industrial and shipping activities, deposition of aerosols and sulfur compounds over the water surfaces is more. Studies show that marine sources like dimethyl sulfide (DMS) (Dixon et al., 2020), oxidation of sulfur compounds in estuarine system (Richards 2016) contribute significantly to atmospheric sulfur levels affecting air quality. Additionally, high levels of AOD concentration are found over coastal waterbodies due to multiple factors including wave breaking and bursting of sea salt aerosols (Ackerman et al., 2023), industrial emission, water traffic, coal combustion (Yan et al., 2017). Furthermore, the proximity to the coast enhances the production of surf-zone aerosols which are transported significant distances over the sea, especially during high wind speeds and wave events (Tedeschi et al., 2017). This also plays a role in elevating the concentration levels of AOD over coastal waterbodies.

The study evaluated the concentration of different air quality parameters of different concentric zones from Payra port and power plant area. It was found that average high level of concentration of all air quality parameters was observed within the immediate vicinity (within 3-kilometer radius) from major infrastructure in the study area. As the distance increased the concentration levels decreased with some exception in certain years. This phenomenon is indicative a typical dispersion pattern associated with the point source of emission.

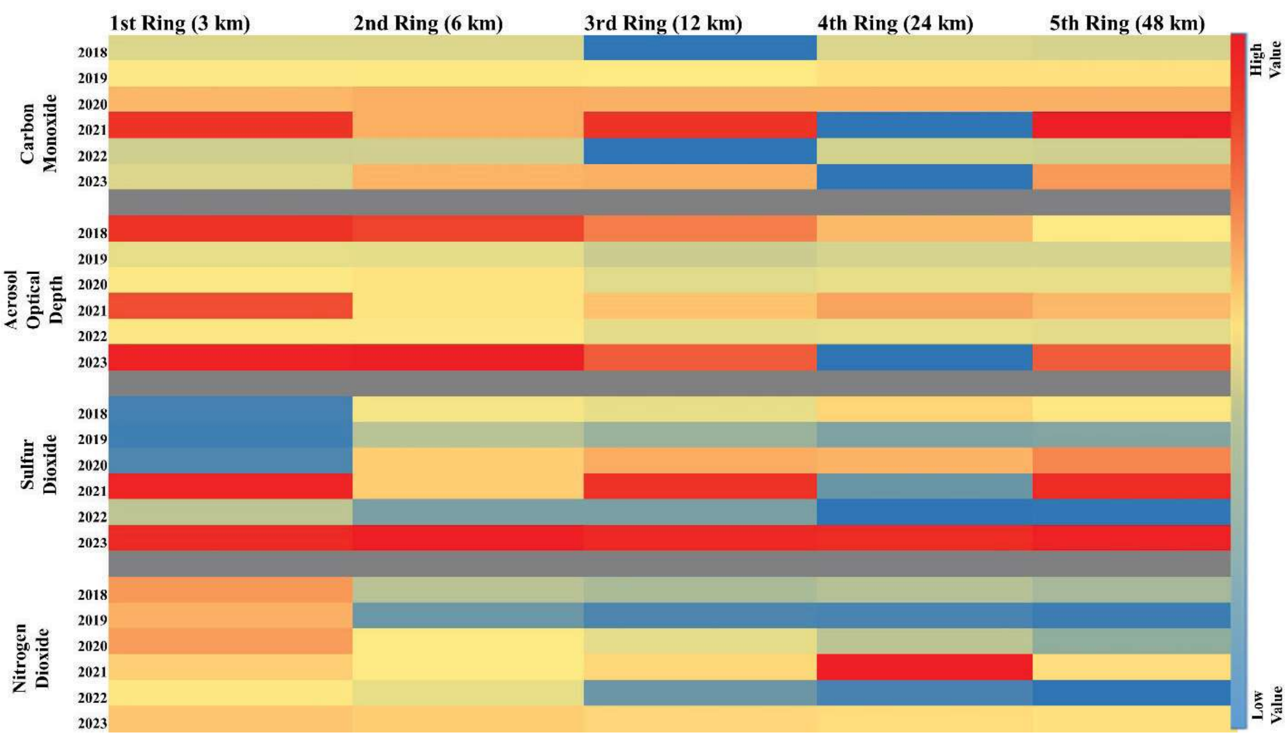

Figure 14: Heat Map Analysis of NO_2, SO_2, CO, and AOD Concentrations across Various Influence Zones

Sulfur dioxide, Carbon Monoxide and Aerosol concentration over the study area especially around 3 kilometer over port and power plant area showed a gradual increase over the years. However, in case of Nitrogen dioxide the concentration levels seemed to have decreased over the same region. Sulfur dioxide concentration. The power plant in the region went into commercial operation from 15th May, 2020 (BCPCL, 2020) and the port started limited commercial operation in August 2016 (PPA, 2022) which may have impacted the heightened level of concentration of different air pollutants in its close proximity. The heat map (Figure

14) frequent fluctuation of concentration levels for different pollutants across different buffer rings over the years. The reasons behind these fluctuations can be better understood through in-depth analysis on a micro scale.

CONCLUSIONS

This study thoroughly examines the air quality dynamics in the south-central coastal area of Bangladesh over six years, specifically focusing on pollutants such as NO_2, SO_2, AOD, and CO. Utilizing a GIS-RS integrated approach proved instrumental in assessing air quality variations. The study investigates the relation between air quality parameters and land cover, revealing higher pollutant concentrations in the northern, western, and central zones. Understanding the complex interplay of local sources, meteorological conditions, land use patterns, and regulatory measures is crucial in deciphering air quality dynamics and development interactions. The findings highlight seasonal variations, with winter increasing human-related emissions and monsoon season indicating elevated pollutants from maritime activities. Integrating GIS and remote sensing technologies allows for a detailed examination of air quality parameters and their correlation with urban development as analysis revealed concentration levels over built environment was higher compared to other classes. However, in order to understand the reason behind the fluctuation of concentration levels across different concentric zones marked in the study requires micro scale analysis. Apart from that, validating the results with field-based data collection of different air quality parameters would've made the study more comprehensive. Despite these limitations, the study addresses a significant gap in understanding coastal air pollution in Bangladesh, emphasizing on its seasonal variation and establishing its relationship with different land cover classes. The insights gained contribute to a broader conversation on sustainable coastal development, urging a balanced approach for healthier ecosystems and communities. Further research is essential to unravel underlying mechanisms and causative factors for sustainable coastal development and community well-being. Future research could incorporate micro scale analysis to pinpoint the pollution sources and integrate ground-based monitoring for proper validation. Linking, pollutant data with health outcomes, cross-regional studies of similar areas would also enable findings that can be actionable for both environment protection and public health policy.

REFERENCES

Ackerman, K. L., Nugent, A. D., Taing, C., 2023. Mechanisms controlling giant sea salt aerosol size distributions along a tropical orographic coastline. https://doi.org/10.5194/egusphere-2023-1387

Ahasan, M. N., Chowdhary, M. A. M., Quadir, D. A., 2010. Variability and trands of summer monsoon rainfall over Bangladesh. Journal of Hydrology and Meteorology 7: 1-17. https://doi.org/10.1016/j.pce.2021.103074

Ahmed, A., Bin Ali, A. A., Mahboob, M., Humaira, F., 2023. Comparison between local and global methods to develop AQI in representing the spatial pattern of air quality of Dhaka City. The Dhaka University Journal of Earth and Environmental Sciences 11(1), 131–149. https://doi.org/10.3329/dujees.v11i1.63716

Akhter, M. S., Das, T. K., 2019. Air pollution in coastal cities of Bangladesh: A review. Environment, Development and Sustainability 21(2), 693-712.

Al-Alola, S. S., Alkadi, I. I., Alogayell, H. M., Mohamed, S. A., Ismail, I. Y., 2022. Air quality estimation using remote sensing and GIS-spatial technologies along Al-Shamal Train Pathway, Al-Qurayyat City in Saudi Arabia. Environmental and Sustainability Indicators 15, 100184. https://doi.org/10.1016/j.indic.2022.100184

Arif, M. T., Siddique, M. A. B., Islam, M. R., 2019. Air pollution in Bangladesh: Status and challenges. Environmental Science and Pollution Research 26(8), 6977-6988.

Arif, M. T., Siddique, M. A. B., Islam, M. R., 2019. Air pollution in Bangladesh: Status and challenges. Environmental Science and Pollution Research 26(8), 6977-6988.

Arif, M., Alam, M. M., Hossain, M. A., 2019. Coastal air pollution in Bangladesh: Sources and mitigation strategies. Environmental Science and Pollution Research 26(35), 35684-35698.

Auvee, M.S., 2019. Air pollution monitoring system based on air pollutant index(API) and geographic information system (GIS).

Ayyam, V., Palanivel, S., Chandrakasan, S., 2019a. Balancing development and environmental impact in the coastal regions. Coastal Ecosystems of the

Tropics - Adaptive Management 579–595. https://doi.org/10.1007/978-981-13-8926-9_25

Ayyam, V., Palanivel, S., Chandrakasan, S., 2019b. Coastal regions of the tropics: An introduction. Coastal Ecosystems of the Tropics - Adaptive Management, 3–20. https://doi.org/10.1007/978-981-13-8926-9_1

BCPCL, 2020. Annual Report 2020 Bangladesh-China Power Company Limited.

Belousov, S. K., Tikunov, V. S., 2022. Assessment and mapping of atmospheric air quality in Russian regions using Earth Remote Sensing Materials. Geodesy and Cartography 988(10), 29–39. https://doi.org/10.22389/0016-7126-2022-988-10-29-39

Bencs, L., Horemans, B., Buczyńska, A. J., Deutsch, F., Degraeuwe, B., Van Poppel, M., Van Grieken, R., 2020. Seasonality of ship emission related atmospheric pollution over coastal and open waters of the North Sea. Atmospheric Environment. X, 7, 100077. https://doi.org/10.1016/j.aeaoa.2020.100077

Chakraborty, J., Armstrong, M.P., 1997. 'Exploring the use of buffer analysis for the identification of impacted areas in environmental equity assessment', Cartography and Geographic Information Systems 24(3), pp. 145–157. doi:10.1559/152304097782476951.

Chakraborty, J., Maantay, J. A., Brender, J. D., 2011. Disproportionate proximity to environmental health hazards: Methods, models, and measurement. American Journal of Public Health 101, S27-S36. https://doi.org/10.2105/AJPH.2010.300109

Chitrakar, P., Baawain, M. S., Sana, A., Al-Mamun, A., 2019. Current status of marine pollution and mitigation strategies in Arid Region: A detailed review. Ocean Science Journal 54(3), 317–348. https://doi.org/10.1007/s12601-019-0027-5

Chowdhury, H., Chowdhury, T., Sait, S. M., 2021. Estimating marine plastic pollution from covid-19 face masks in coastal regions. Marine Pollution Bulletin 168, 112419. https://doi.org/10.1016/j.marpolbul.2021.112419

Collins, S., 2020. Modelling urban air pollution using GIS. Geographic Information Research 427–440. https://doi.org/10.1201/9781003062691-33

Dai, C., Han, Y., Duan, Y., Lai, X., Fu, R., Liu, S., Leong, K. H., Tu, Y., Zhou, L., 2022. Review on the contamination and remediation of polycyclic aromatic hydrocarbons (pahs) in coastal soil and sediments. Environmental Research 205, 112423. https://doi.org/10.1016/j.envres.2021.112423

Dhankar, S., Singh, G., Kumar, K., 2024. Impact of Urbanization on Air Quality of Dehradun District. Current World Environment/Current World Environment 19(1), 321–337. https://doi.org/10.12944/cwe.19.1.27

Dixon, J. L., Hopkins, F. E., Stephens, J. A., Schäfer, H., 2020. Seasonal changes in microbial dissolved organic sulfur transformations in coastal waters. Microorganisms 8(3), 337. https://doi.org/10.3390/microorganisms8030337

Faisal, A.-A.-, Rahman, M. M., Haque, S., 2022. Retrieving spatial variation of aerosol level over urban mixed land surfaces using landsat imageries: Degree of air pollution in Dhaka metropolitan area. Physics and Chemistry of the Earth, Parts A/B/C 126, 103074.

Hasan, M. M., Ahmed, A., 2023. Evaluation and mapping the atmospheric air quality of coastal area in Bangladesh using remote sensing and GIS techniques. The Dhaka University Journal of Earth and Environmental Sciences 11(2), 53–64. https://doi.org/10.3329/dujees.v11i2.68840

Hu, M., Guo, Q., Shang, D., Wu, Z., Lu, S., Guo, S., 2023. Regional transport and formation of air pollutants between sea and land under the monsoon climate. https://doi.org/10.5194/egusphere-egu23-2334

JMPDLB, N. J., Elangasinghe, N., 2022. Air quality improvement during COVID-19 lockdown in colombo, Sri Lanka. Proceedings of the International Forestry and Enviroment Symposium 26. https://doi.org/10.31357/fesympo.v26.5698

Khatun, M. A., RASHID, M. B., Hygen, H. O., 2016. Climate of Bangladesh. Technical report, Norwegian Meteorological Institute, 1-158

Lucas, R., Rowlands, A., Brown, A., Keyworth, S., Bunting, P., 2007. Rule-based classification of multi-temporal satellite imagery for habitat and agricultural land cover mapping. ISPRS Journal of Photogrammetry and Remote Sensing 62(3), 165-185. https://doi.org/10.1016/j.isprsjprs.2007.03.003

Magesh, N. S., Ch, N., 2012. A GIS based automated extraction tool for the analysis of basin morphometry. Bonfring International Journal of Industrial Engineering and Management Science, 2(Special Issue Special Issue on Geospatial Technology Development in Natural Resource and Disaster Management) 32-35. http://www.journal.bonfring.org/abstract.php?id=3&archiveid=144

Mikhaylova, A. A., Gorochnaya, V. V., Gumenyuk, I. S., Plotnikova, A. P., Mikhaylov, A. S., 2021. Does the coastal location of municipalities influence their innovation development? Vestnik of Saint Petersburg University. Earth Sciences 66(3). https://doi.org/10.21638/spbu07.2021.303

Mogno, C., Palmer, P. I., Knote, C., Yao, F., Wallington, T. J., 2021. Seasonal distribution and drivers of surface fine particulate matter and organic aerosol over the Indo-Gangetic Plain. Atmospheric Chemistry and Physics 21(14), 10881–10909. https://doi.org/10.5194/acp-21-10881-2021

Oikawa, P. Y., Ge, C., Wang, J., Eberwein, J. R., Liang, L. L., Allsman, L. A., Grantz, D. A., Jenerette, G. D., 2015. Unusually high soil nitrogen oxide emissions influence air quality in a high-temperature agricultural region. Nature Communications, 6(1). https://doi.org/10.1038/ncomms9753

Pavel, M. R., Zaman, S. U., Jeba, F., Islam, M. S., Salam, A., 2021. Long-term (2003–2019) air quality, climate variables, and human health consequences in Dhaka, Bangladesh. Frontiers in Sustainable Cities 3. https://doi.org/10.3389/frsc.2021.681759

Pavithran, V. A., 2021. Study on microplastic pollution in the coastal seawaters of selected regions along the northern coast of Kerala, southwest coast of India. Journal of Sea Research 173, 102060. https://doi.org/10.1016/j.seares.2021.102060

Piazzolla, D., Della Ventura, G., Terribili, A., Conte, A., Scanu, S., Bonamano, S., Marcelli, M., Lucci, F., La Bella, C., Venettacci, C., 2021. Air pollution assessment using a cost-effective device: The case study of the northern latium Coastal Area. https://doi.org/10.5194/egusphere-egu21-10223

Piscopo, A., Galdies, C., Gauci, A., 2022. Assessing the air quality derived from marine traffic in the Central Mediterranean and Malta. IGARSS 2022 - 2022 IEEE International Geoscience and Remote Sensing Symposium. https://doi.org/10.1109/igarss46834.2022.9883392

PPA, 2022. Payra Port Authority. Available at: https://ppa.gov.bd/site/page/0d44bdb6-9468-4d3b-b0de-d1ebb3fabc7c/Welcome-to-Payra-Port-Authority (Accessed: 17 July 2024).

Qi, J., Wang, S., Qu, X., 2020. Emission evaluation of marine traffic, Smart Transportation Systems 2020, 201–211. doi:10.1007/978-981-15-5270-0_18.

Qiu, Z., Ali, Md. A., Nichol, J. E., Bilal, M., Tiwari, P., Habtemicheal, B. A., Almazroui, M., Mondal, S. K., Mazhar, U., Wang, Y., Sarker, S., Mustafa, F., Rahman, M. A., 2021. Spatiotemporal investigations of multi-sensor air pollution data over Bangladesh during COVID-19 lockdown. Remote Sensing 13(5), 877. https://doi.org/10.3390/rs13050877

Rajkumar R., Elangovan K., Navinganesh V., Govarthanambikai, K., 2023, Assessment of urban air quality using geo spatial techniques for sustainable development: case of Tirupur City, India, Global NEST Journal 25(5), 147-152

Rawat, J. S., Kumar, M., 2015. Monitoring land use/cover change using remote sensing and GIS techniques: A case study of Hawalbagh block, district Almora, Uttarakhand, India. The Egyptian Journal of Remote Sensing and Space Science 18(1), 77-84. https://doi.org/10.1016/j.ejrs.2015.02.002

Richards, C. M., 2016. Biogeochemical sulfur cycling in the bar-built Pescadero Estuary: Interdisciplinary investigations into near-annual fish mortality events.

Richards, CM., 2016. Biogeochemical sulfur cycling in the bar-built Pescadero Estuary: Interdisciplinary investigations into near-annual fish mortality events.

Sahu, P. C., Tripathy, P. P., Mohanty, B., 2019. A review on air pollution from coal-fired power plants. Journal of Environmental Management 235, 576-586.

Salam, A., Andersson, A., Jeba, F., Haque, Md. I., Hossain Khan, M. D., Gustafsson, Ö., 2021. Wintertime air quality in megacity Dhaka, Bangladesh strongly affected by influx of black carbon aerosols from regional biomass burning. Environmental Science andamp; Technology 55(18), 12243–12249. https://doi.org/10.1021/acs.est.1c03623

Siudek, P., 2020. Seasonal variability of trace elements in fine particulate matter (PM2.5) in a coastal city of northern Poland – profile analysis and source identification. Environmental Science. Processes & Impacts. https://doi.org/10.1039/d0em00031k

Su, X., He, C., Feng, Q., Deng, X., Sun, H., 2010. A supervised classification method based on conditional random fields with multiscale region connection calculus model for SAR image. IEEE Geoscience and Remote Sensing Letters 8(3), 497-501.

Talib, A. M., Jasim, M. N., 2021. Withdrawn: GIS-GPS based National Air Pollution Monitoring System. Materials Today: Proceedings. https://doi.org/10.1016/j.matpr.2021.05.445

Tareq, N. a. M., Shaikh, N. M. A., Sen, N. S., Xuefeng, N. P. W., 2020. Deep sea port and the national development: Perspective of Bangladesh. International Journal of Engineering and Management Research 10(6), 73–80. https://doi.org/10.31033/ijemr.10.6.11

Tedeschi, G., Van Eijk, A. M. J., Piazzola, J., Kusmierczyk-Michulec, J. T., 2017. Influence of the surf zone on the marine aerosol concentration in a Coastal Area. Boundary-layer Meteorology/ Boundary - Layer Meteorology 163(2), 327–350. https://doi.org/10.1007/s10546-016-0229-7

Wang, T., Cheung, T. F., Li, Y. S., Yu, X. M., Blake, D. R., 2002. Emission characteristics of CO, NOx, SO2 and indications of biomass burning observed at a rural site in eastern China. Journal of Geophysical Research 107(D12). https://doi.org/10.1029/2001jd000724

Wei, M., Li, M., Xu, C., Xu, P., Liu, H., 2020. Pollution characteristics of bioaerosols in PM2.5 during the winter heating season in a coastal city of northern China. Environmental Science and Pollution Research International 27(22), 27750–27761. https://doi.org/10.1007/s11356-020-09070-y

Williams, B. A., Watson, J. E., Beyer, H. L., Klein, C. J., Montgomery, J., Runting, R. K., Roberson, L. A., Halpern, B. S., Grantham, H. S., Kuempel, C. D., Frazier, M., Venter, O., Wenger, A., 2021. The Global Rarity of Intact Coastal Regions. https://doi.org/10.1101/2021.05.10.443490

Williams, B. A., Watson, J. E., Beyer, H. L., Klein, C. J., Montgomery, J., Runting, R. K., Roberson, L. A., Halpern, B. S., Grantham, H. S., Kuempel, C. D., Frazier, M., Venter, O., Wenger, A., 2021. The Global Rarity of Intact Coastal Regions. https://doi.org/10.1101/2021.05.10.443490

Yan, J. P., Chen, L. Q., Lin, Q., Zhao, S. H., Li, L., Zhu, D. Y., 2017. Marine aerosol using on-board aerosol mass spectrometry. PubMed 38(7), 2629–2636. https://doi.org/10.13227/j.hjkx.201612065

Zaman, S. U., Pavel, Md. R., Joy, K. S., Jeba, F., Islam, Md. S., Paul, S., Bari, Md. A., Salam, A., 2021. Spatial and temporal variation of aerosol optical depths over six major cities in Bangladesh. Atmospheric Research 262, 105803. https://doi.org/10.1016/j.atmosres.2021.105803

Zha, Y., Gao, J., Ni, S., 2003. Use of normalized difference built-up index in automatically mapping urban areas from TM imagery. International Journal of Remote Sensing 24(3), 583-594. https://doi.org/10.1080/01431160304987